SUPPLEMENTARY FIGURES

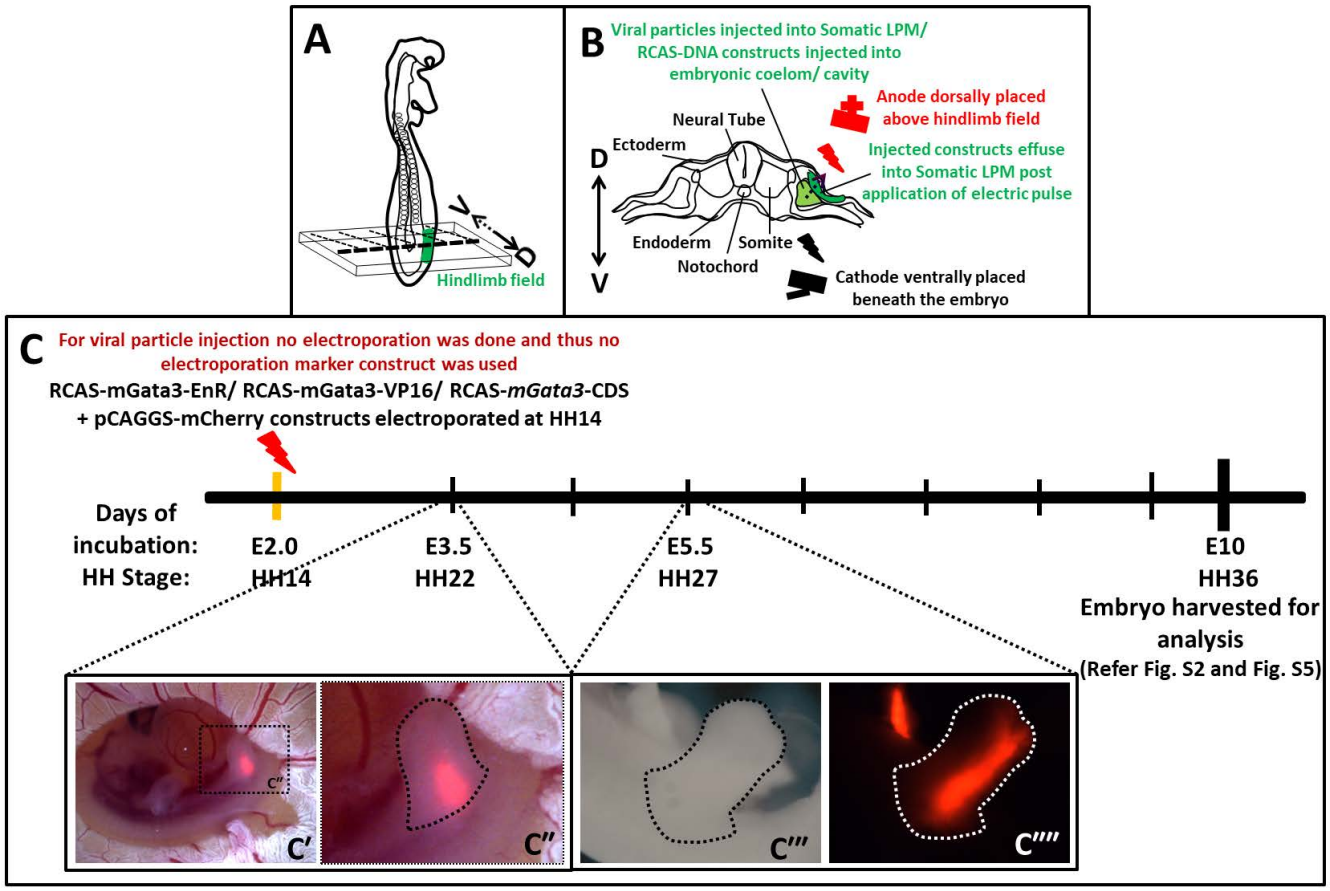

Fig. S1. Schematic representation of the experiments carried out in this study. (A) In a HH14 stage chick embryo limb fields are recognized as small protuberances at specific locations along the body wall of the embryo or LPM (lateral plate mesoderm). Hindlimb field is marked in green. (B) A transverse section of the limb field represented in (A) along the dorso-ventral (D-V) axis. At stage HH14 the DNA constructs or retroviral particles, mixed with 0.1% fast green, was injected into the embryonic space between the somatic LPM and splanchnic LPM at a concentration of 2µg/µl using a microinjector. Post-microinjection electroporation is performed if DNA construct was injected. As soon as the DNA was injected platinum cathode was placed within the albumin beneath the yolk sac while an L-shaped anode was placed in parallel to the embryo over the hindlimb field before electric pulses (10V, 50ms pulse-on, 950ms pulse-off, five repetitions) were applied. Injected constructs get inside the nucleus of the cells on the dorsal side of the LPM, called the somatic LPM which eventually gives rise to limb buds as represented in (C″). (C) Timeline of the experimental setup. At stage HH14 RCAS construct RCAS-*mGata3*-CDS or RCAS-GATA3DBD-VP16 or RCAS-GATA3DBD-EnR mixed with 0.5µg/µl pCAGGS-mCherry was electroporated as represented in panel (B). (C′) At stage HH22 expression of mCherry within the limb bud indicates successful electroporation. (C″) Magnified image of the hindlimb region marked in (C′) represents the mCherry expression within the limb bud. (C‴) represents mCherry expression at day5.5 i.e. HH27. (C‴) is the bright-filed image of the same limb bud. All the embryos analysed in this study were harvested at HH36.

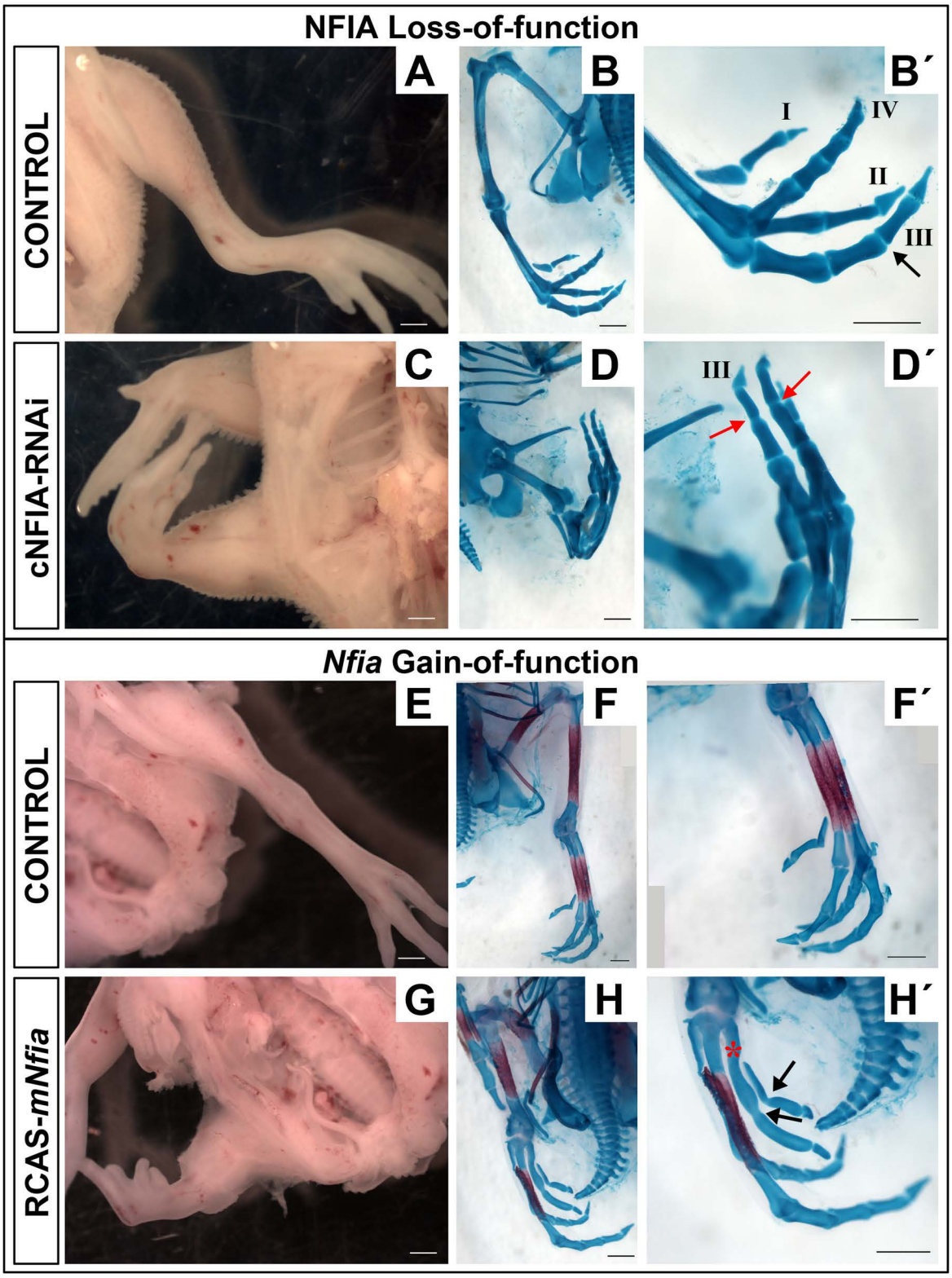

Fig. S2. Skeletal prep analysis of RCAS-cNFIARNAi and RCAS-m*Nfia* infected limbs compared to respective uninfected contralateral control limbs. Whole mount view of unfixed, unstained RCAS-cNFIARNAi infected limb (C) compared with uninfected contralateral control (A) at HH36. (B) Alcian blue stained uninfected contralateral control limb, (B′) shows magnified view of the phalangeal region where black arrow marks the segmented joint between the second and the third phalanx in the third digit. (D) Alcian blue stained RCAS-cNFIA-shRNAi infected limb, (D′) shows magnified view of the phalangeal region where red arrow marks the unsegmented joint between the second and the third phalanx in the third digit. Whole mount view of unfixed, unstained RCAS-m*Nfia* infected limb (G) compared with uninfected contralateral control (E) at HH36. (F) Alcian blue-alizarin red stained uninfected contralateral control limb and (F′) shows magnified view of the meta-tarsus. (H) Alcian blue-alizarin red stained RCAS-m*Nfia* infected limb and (H′) shows magnified view of the meta-tarsus, arrows marks the unsegmented skeletal elements, red asterisk marks the element showing reduced alizarin red staining. Scale bar- 1mm.

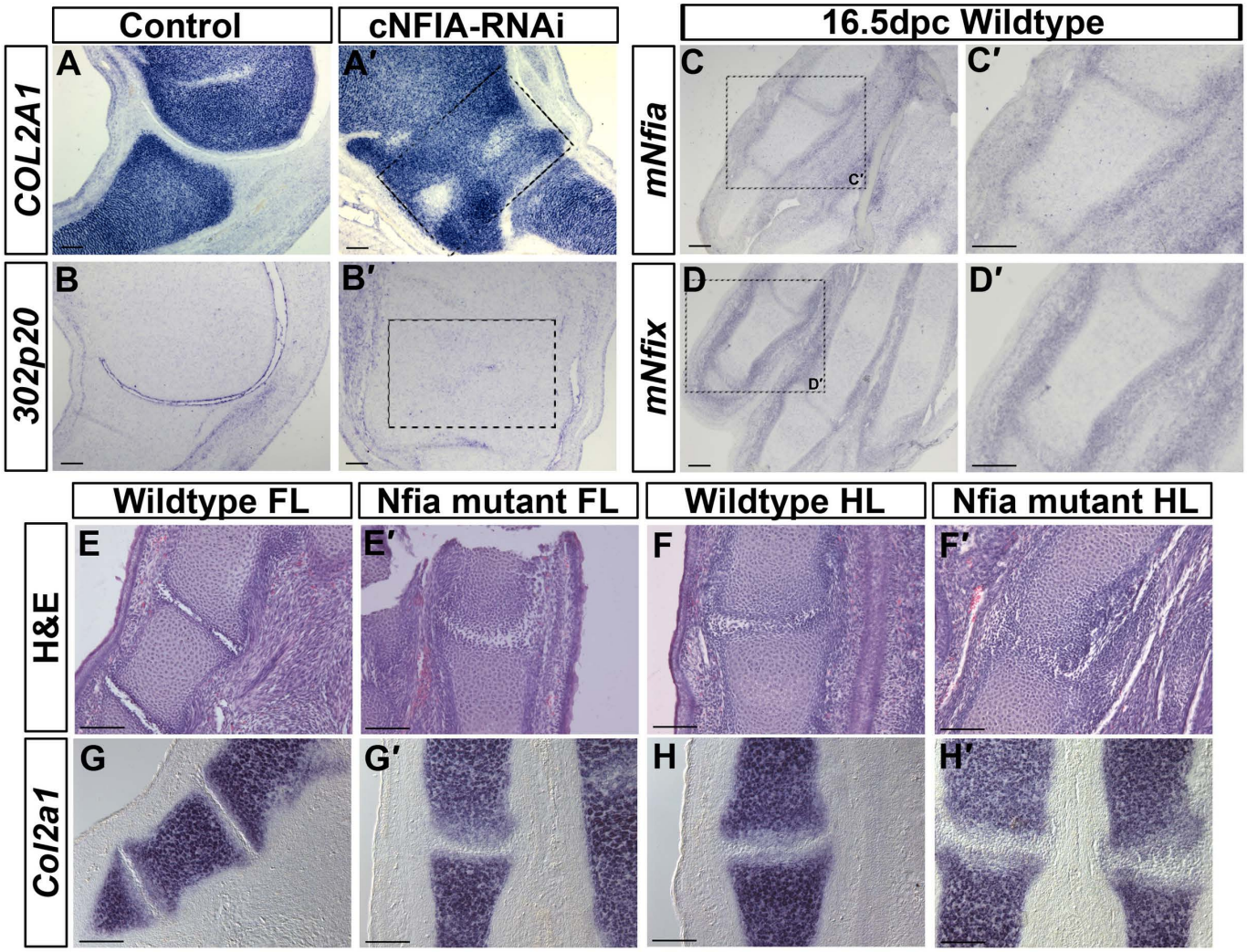

Fig. S3.NFIA loss-of-function leads to loss of interzone markers. (A,B) represent tibio-tarsal joint of an uninfected contralateral control limb and (A′,B′) represent RCAS-*cNFIA-RNAi* infected tibio-tarsal joint region. RNA *in situ* hybridization images for *COL2A1* (A and A′), *ChEST302p20* (B and B′). (C and D) RNA *in situ* hybridization images for*m Nfia* and *mNfix* respectively, (C′ and D′) shows magnified region from (C and D). (E-H) MTP joint of WT control and (E′-H′) *Nfia* mutant limbs. (E, E′, F and F′) Hematoxylin and Eosin staining. (G, G′, H and H′) RNA *in situ* hybridization for mouse *Col2a1*.Scale bar- 100 µm.

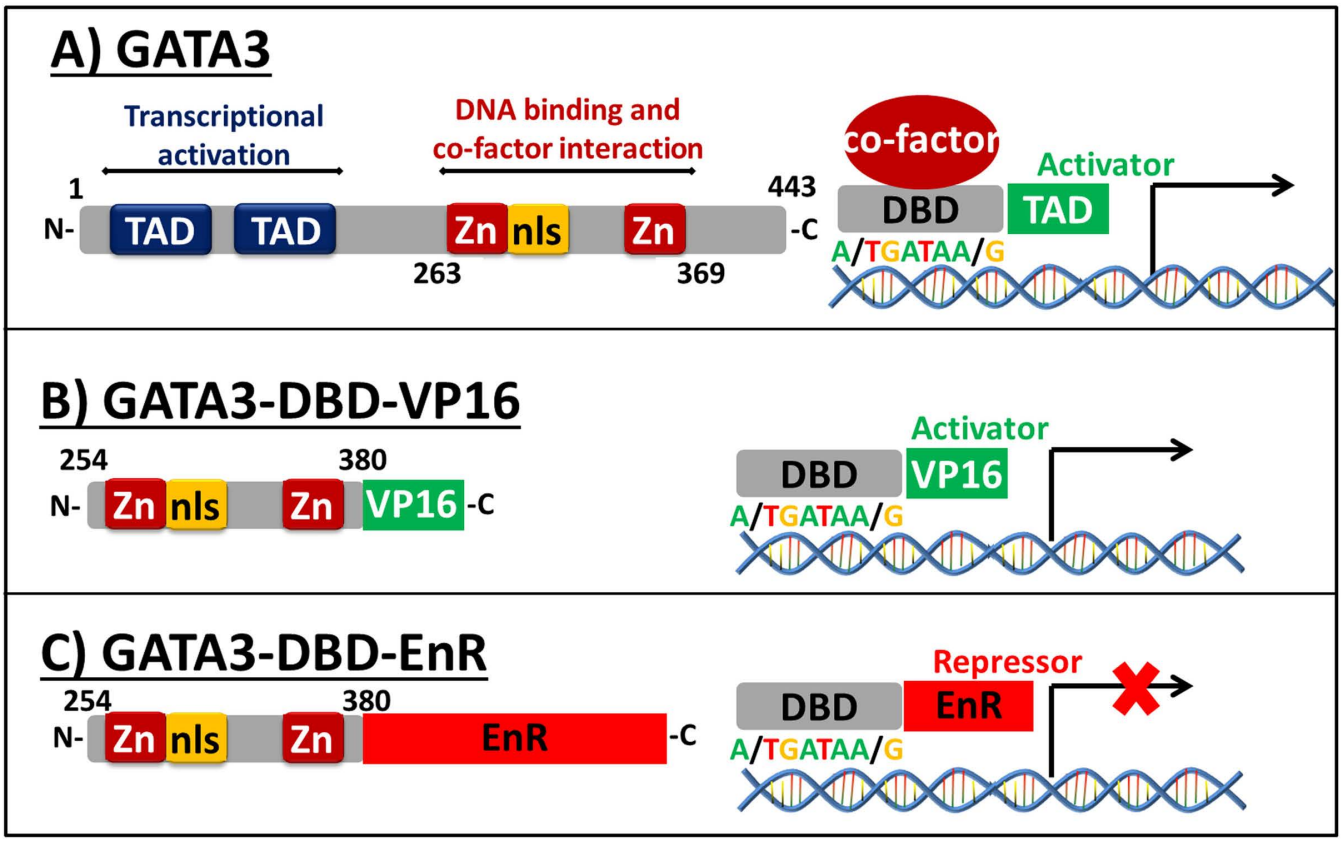

Fig. S4. Strategy adopted for generation of Gata3 gain-of-function and loss-of-function constructs. (A) Represents a full length mouse-GATA3 protein comprising of two amino-terminal transactivation domains followed by two zinc finger domains. (B) GATA3-DBD-V16 represents a constitutively active form of GATA3 generated by fusion of an in-frame strong trans-activator VP16 at the C-terminus of mGATA3 DNA binding domain. Thus constitutively transcribing the genes modulated by GATA3 binding. (C) GATA3-DBD-EnR represents a constitutively active form of GATA3 generated by fusion of an in-frame strong repressor EnR at the C-terminus of mGATA3 DNA binding domain. Thus constitutively repressing the genes modulated by GATA3 binding. The constructs were made as per method described by Kamei etet. al. (2011).

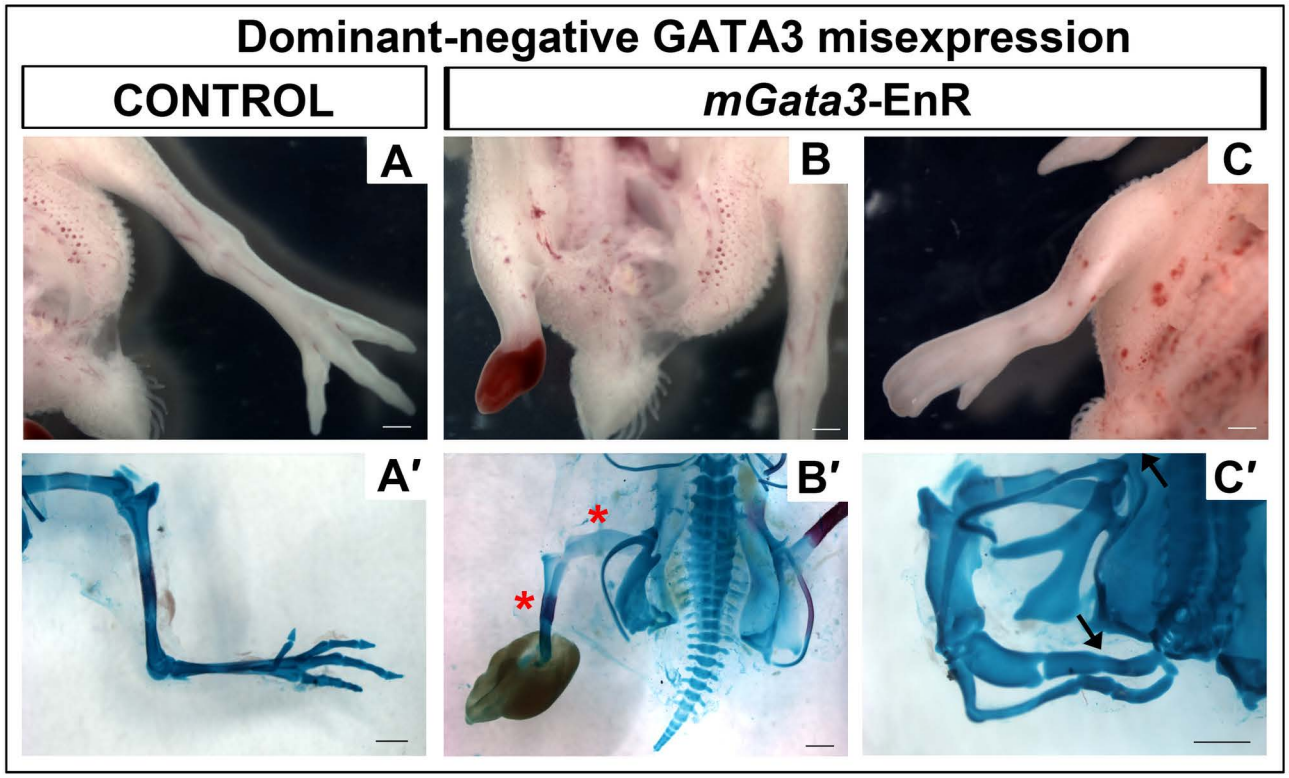

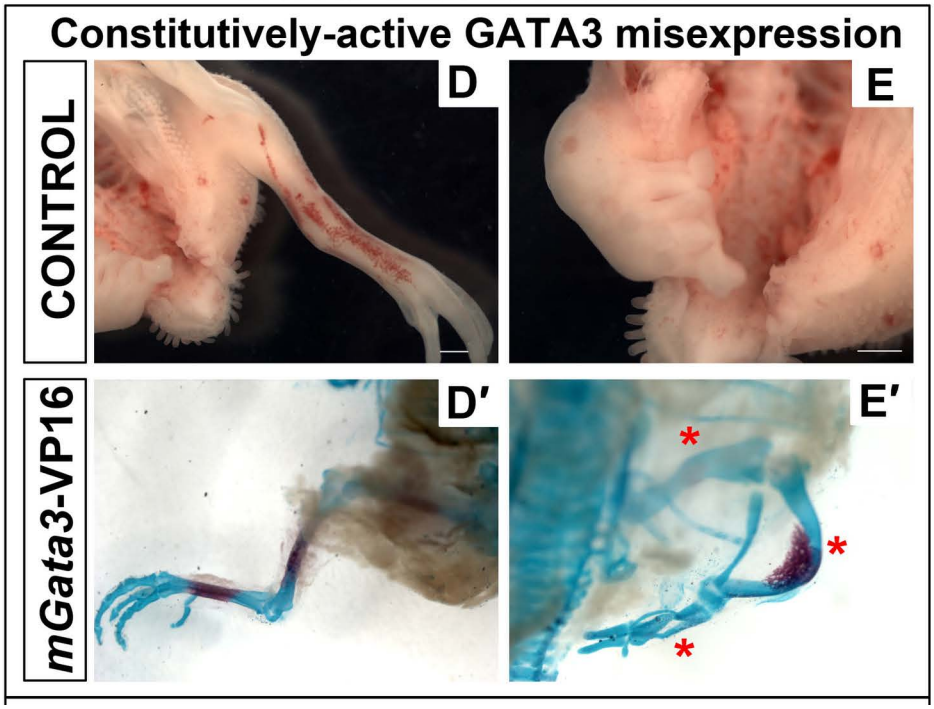

Fig. S5. *Gata3*-EnR and *Gata3*-VP16 infected limbs compared to respective uninfected contralateral control limbs. Whole mount view of unfixed, unstained RCAS-*Gata3*-EnR infected limb (B and C) and uninfected contralateral limb (A) at HH36. Alcian blue-alizarin red stained uninfected contralateral control limb (A′) and RCAS-*Gata3*-EnR infected limb with severe (B′) to less severe (C′) skeletal deformity. Arrows mark the unsegmented skeletal elements; red asterisks mark the elements showing reduced alizarin red staining. Whole mount view of unfixed, unstained RCAS-*Gata3*-VP16 infected limb (E) and uninfected contralateral limb (D) at HH36. Alcian blue-alizarin red stained whole mount skeletons from (D′) uninfected contralateral control limb and (E′) RCAS-*Gata3*-VP16 infected limb, where red asterisks mark the elements showing reduced alizarin red staining. Scale bar- 1mm.

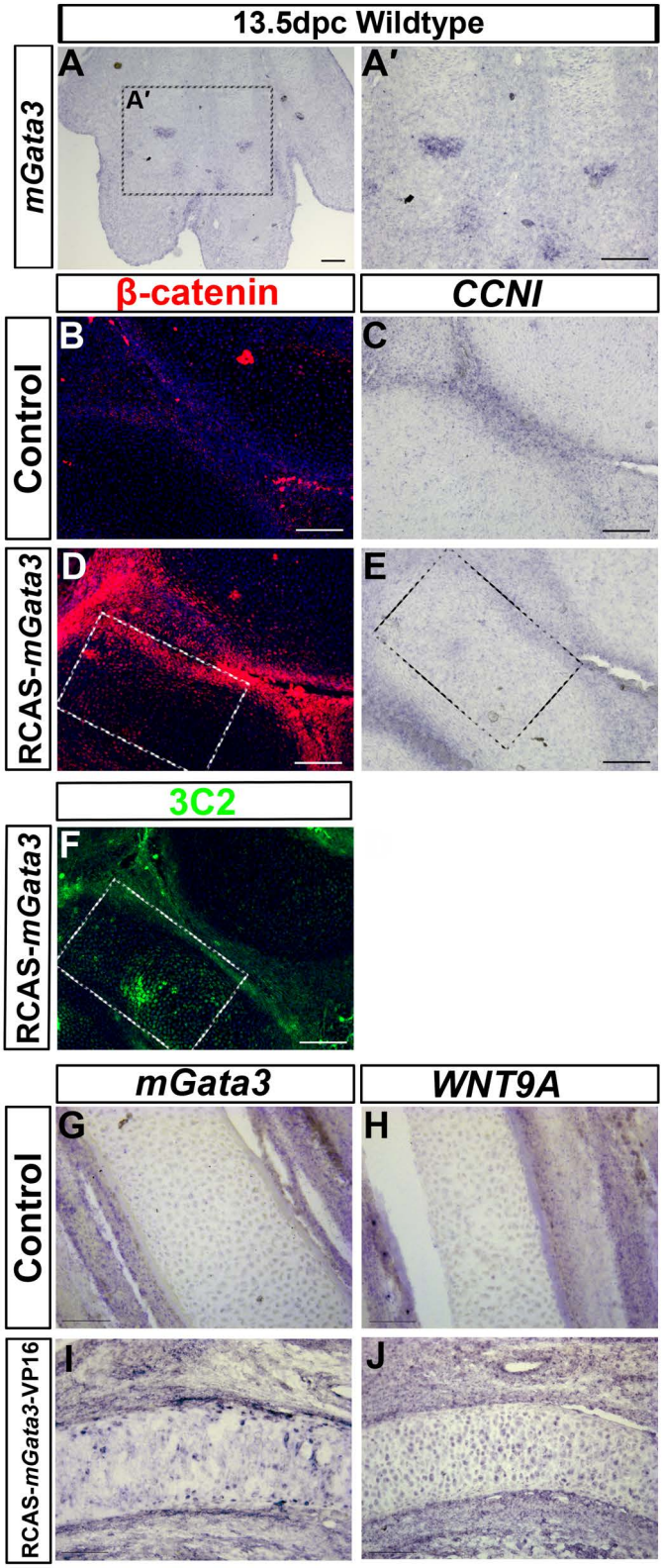

Fig. S6. Gata3 gain-of-function. (A) Expression of mouse *Gata3* mRNA in 13.5dpc mouse hindlimb digits. (A′) Magnified view of the boxed region in Panel A. (B-F) CCNI, an articular cartilage specific gene, is not overexpressed when mGata3 is virally misexpressed. (B and C) represent endogenous level of β-catenin immuno-reactivity (B) and CCNI mRNA expression (C) in tibio-tarsal joint of an uninfected contralateral control chick limb. (D and E) β-catenin immuno-reactivity (D), and CCNI mRNA expression (E), in the RCAS-m*Gata3*-cDNA infected HH36 tibio-tarsal joint region. (F) Immunohistochemistry with 3C2 (antibody against the viral gag protein) on a section serial to the ones used in panels D and E marks the viral infection domain in green within the boxed region. (G-J) Overexpression of mGata3-VP16 causes ectopic expression of Wnt9a. (G) RNA *in situ* hybridization against *mGata3* in non-infected contralateral control tibia. (H) RNA *in situ* hybridization against *WNT9A* in non-infected contralateral control tibia. (I) RNA *in situ* hybridization against mGata3 highlights the mGata3-VP16 infected tibia. (J) Ectopic expression of Wnt9a in the mGata3-VP16 infected tibia. I and J are serial sections. Scale bar- 100 µm.

Table S1: Articular cartilage specific genes that were identified as transcriptional targets of Gata3 in the microarray profiling performed by Kourous-Mehr et al. (2006).

ID_REF	VALUE	Avalue	Description	Symbol
22436	3.019	9.499	ectonucleotide pyrophosphatase/phosphodiesterase 2 (Atx)	Enpp2
36565	1.904	9.611	cyclin I	CCNI
11991	1.364	8.416	hypoxia inducible factor 1, alpha subunit	HIF1A
29726	1.112	9.046	cadherin 11	CDH11
14359	0.889	10.04	fibulin 1	FBLN1
18280	0.685	8.686	tenascin C	TNC
7418	0.412	12.638	growth differentiation factor 5	GDF5
13997	0.384	9.399	chordin	CHRD
12648	0.356	15.331	insulin-like growth factor binding protein 4	IGFBP4
12398	0.351	11.785	wingless-type MMTV integration site 9A	Wnt9a
31109	0.268	10.412	secreted frizzled-related sequence protein 2	SFRP2
27708	0.226	15.643	clusterin	CLU
13437	0.214	11.113	chondroitin sulfate proteoglycan 2 (versican)	CSPG2
35186	0.189	10.053	nuclear factor I/A	NFIA
14761	0.07	8.062	GLI-Kruppel family member GLI3	GLI3
8289	0.016	12.726	catenin (cadherin associated protein), beta 1, 88kDa	CTNNB1

#ID_REF = Unique Identifier
#VALUE = Lowess M Log Ratio (F635 Median, F532 Median), $\log_2$(Het /Null) where Het = fluorescence intensity of WAP-rtTA-Cre;GATA-3$^{flox/+}$sample and Null = fluorescence intensity of WAP-rtTA-Cre;GATA-3$^{flox/flox}$ sample
#Avalue = Lowess A Log Ratio (F635 Median, F532 Median)

Supplementary Table 2: List of clones used

Genes	**ChEST ID/ Source**
SFRP2	ChEST712d9
Atx	ChEST520a5
c-Jun	ChEST520g15
ERG	Cloned
PTHRP	Minina et al., 2001
NFIA *Nuclear factor I/A*	ChEST864l9
mNFIA	Deneen et al., 2006
mNFIX	IRAV 3491917
mGATA3	Kamei et al.,2011
PHLDA2 *Pleckstrin homology-like domain, family A, member 2*	ChEST533e11
Finished cDNA clone ChEST302p20	ChEST302p20
CCNI *Cyclin I*	ChEST605d20
GDF5	Hartmann et al., 2001
BMP4	Francis et al., 1994
COL2A1	Hartmann et al., 2001

mCOL2A1	
WNT9a	ChEST592n13
GATA3	ChEST663o17
IHH	Minina et al., 2001
PTHrPR	Minina et al., 2001

Hartmann C, Tabin CJ. 2001. Wnt-14 plays a pivotal role in inducing synovial joint formation in the developing appendicular skeleton. Cell 104:341-351.

Minina E, Wenzel HM, Kreschel C, Karp S, Gaffield W, McMahon AP, Vortkamp A. 2001. BMP and Ihh/PTHrP signaling interact to coordinate chondrocyte proliferation and differentiation. Development 128:4523-4534.

Kamei, C. N., Kempf, H., Yelin, R., Daoud, G., James, R. G., Lassar, A. B., Tabin, C. J., and Schultheiss, T. M. (2011). Promotion of avian endothelial cell differentiation by GATA transcription factors. Dev Biol *353*, 29-37.

Deneen, B., Ho, R., Lukaszewicz, A., Hochstim, C. J., Gronostajski, R. M., and Anderson, D. J. (2006). The transcription factor NFIA controls the onset of gliogenesis in the developing spinal cord. Neuron *52*, 953-968.

Francis PH, Richardson MK, Brickell PM, Tickle C. 1994. Bone morphogenetic proteins and a signalling pathway that controls patterning in the developing chick limb. Development 120:209-218.